The Canadian Mineralogist
Vol. 56, pp. 763-772 (2018)
DOI: 10.3749/canmin.1800046

BODIEITE, $Bi^{3+}_2(Te^{4+}O_3)_2(SO_4)$, A NEW MINERAL FROM THE TINTIC DISTRICT, UTAH, AND THE MASONIC DISTRICT, CALIFORNIA, USA

ANTHONY R. KAMPF[§]

Mineral Sciences Department, Natural History Museum of Los Angeles County, 900 Exposition Boulevard, Los Angeles, California 90007, U.S.A.

ROBERT M. HOUSLEY

Division of Geological and Planetary Sciences, California Institute of Technology, Pasadena, California 91125, U.S.A.

GEORGE R. ROSSMAN

Division of Geological and Planetary Sciences, California Institute of Technology, Pasadena, California 91125, U.S.A.

JOE MARTY

5199 East Silver Oak Road, Salt Lake City, Utah 84108, U.S.A.

MAREK CHORAZEWICZ

124 Pineplank Lane, Simi Valley, California 93065, U.S.A.

ABSTRACT

Bodieite (IMA2017-117), $Bi^{3+}_2(Te^{4+}O_3)_2(SO_4)$, is a new mineral from a dump near the North Star mine, Tintic district, Juab County, Utah, and the Pittsburg-Liberty mine, Masonic district, Mono County, California, U.S.A. It is an oxidation-zone mineral occuring in vugs. Crystals occur in a variety of habits, including bladed, acicular, steep pyramidal, and stepped tabular; they are generally elongate on [001] and exhibit the forms {001}, {110}, {111}, and $\{11\bar{1}\}$. The mineral ranges in color from colorless to yellow to green. The streak is white, the luster is subadamantine to greasy, and crystals are transparent to translucent. The mineral is nonfluorescent under ultraviolet light. The Mohs hardness is about 2, the tenacity is brittle, the cleavage is fair on {001}, and the fracture is irregular, stepped. The calculated density is 6.465 g/cm^3. The mineral is readily soluble in dilute HCl at room temperature. Bodieite is biaxial (–) with all indices of refraction > 2; $2V_{meas} = 71.5°$; orientation X = **b**; nonpleochroic. The Raman spectrum exhibits bands clearly fitting tellurite and sulfate groups. Electron-microprobe analyses gave the empirical formula $(Bi_{1.95}Te_{1.89}As_{0.14}Sb_{0.02})_{\Sigma 4.00}(S_{1.02}O_4)O_6$. The mineral is monoclinic, space group $I2/a$, with a 8.1033(8), b 7.4302(8), c 14.6955(17) Å, β 97.771(9)°, $V = 876.68(16)$ Å^3, and $Z = 4$. The six strongest X-ray powder diffraction lines are [d_{obs} Å(I)(hkl)]: 7.31(20)(002), 3.331(62)(202, $\bar{1}$21), 3.243(100)(121), 3.039(20)($\bar{2}$13), 2.716(25)(220,015), and 1.9013(21)(323). The structure of bodieite contains $Bi^{3+}O_3$ and $Te^{4+}O_3$ pyramids that share O vertices forming an undulating sheet parallel to {001}. Interlayer SO_4 groups link the sheets *via* long Bi–O and Te–O bonds.

Keywords: bodieite, new mineral, tellurium oxysalt, crystal structure, Raman spectroscopy, electron microprobe analysis, Tintic district, Utah, Masonic district, California, USA.

[§] *Corresponding author e-mail address*: akampf@nhm.org

Introduction

Besides bodieite, only four oxysalt minerals are known or suspected to contain both essential Te^{4+} and Bi^{3+}: chekhovichite, $Bi^{3+}{}_2Te_4{}^{4+}O_{11}$, pingguite, $Bi^{3+}{}_6Te_2{}^{4+}O_{13}$, smirnite, $Bi^{3+}{}_2Te^{4+}O_5$, and yecoraite, $Fe_3{}^{3+}Bi^{3+}{}_5(Te^{6+}O_4)_2(Te^{4+}O_3)O_9{\cdot}9H_2O$. Structures have been determined for only two of these, chekhovichite (Rossell *et al*. 1992) and smirnite (Ok *et al*. 2001). Both Te^{4+} and Bi^{3+} generally have stereoactive lone-electron pairs, and this results in off-center cation–oxygen coordinations, with short, stronger bonds on one side of the cation. The most typical such coordination for Te^{4+} involves short bonds to three O atoms to form the pyramidal $(Te^{4+}O_3)^{2-}$ group with Te^{4+} at its apex. This coordination is also common for Bi^{3+}; however, in the structure of chekhovichite, neither of the two Bi^{3+} coordinations are well-defined pyramids and in smirnite only one of three nonequivalent Bi^{3+} cations forms a well-defined pyramidal $(Bi^{3+}O_3)^{3-}$ group. As will be seen below, both the Te^{4+} and Bi^{3+} coordinations in the structure of bodieite are well-defined pyramids, and the strong linkages between these through shared O vertices creates a novel undulating sheet that is the most distinctive feature of the structure.

The mineral is named bodieite (/'boʊ di: aɪt/) for the Bodie Hills volcanic field, in which the Pittsburg-Liberty mine is located, and for the town of Bodie, California, which is about 19 km SSE of the Pittsburg-Liberty mine. Bodie, a gold-mining boomtown established in 1876, had a population of 5000 to 7000 in the late 1870s. Today, the town site is a National Historic Landmark. Bodie State Historic Park, established in 1962, attracts about 200,000 visitors annually. The new mineral and name have been approved by the Commission on New Minerals, Nomenclature and Classification of the International Mineralogical Association (IMA2017-117). Five cotype specimens are deposited in the Natural History Museum of Los Angeles County (900 Exposition Boulevard, Los Angeles, California 90007, USA), catalogue numbers 67482 (dump near North Star mine) and 67483 through 67486 (Pittsburg-Liberty mine).

Occurrence and Paragenesis

The mineral was first recognized as a potentially new species in 2011 by Jerry Baird of Lake Havasu, Arizona, on a specimen that had been collected by John Dagenais of Vancouver, British Columbia, Canada, in 2010, from a small isolated ore dump in the Tintic district, Juab County, Utah, USA (39.921298°, –112.108668°). This dump is about 0.2 km west of the North Star mine but is not directly associated with it. In 2017, Kyle Beucke of San Bruno, California, brought to our attention the occurrence of interesting Bi-Te mineralization at mines in the Masonic district, Mono County, California, USA. This led to the discovery of the mineral by three of the authors (RMH, JM, and MC) on the lower dump of the Pittsburg-Liberty mine (38.358637°, –119.120321°) in the Masonic district. The mine is about 19 km NNW of Bodie, Mono County, California, USA. These two occurrences provided the material used for the characterization of this new species.

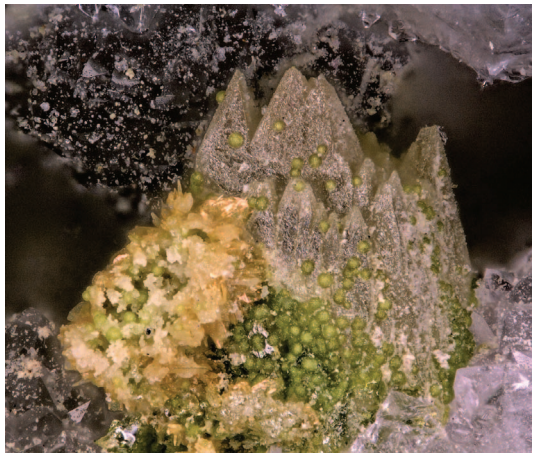

Fig. 1. Bodieite, green richelsdorfite, and yellow unknown on quartz from the Pittsburg-Liberty mine; FOV 1 mm.

The material on the small isolated dump west of the North Star mine does not closely resemble material collected from the dumps directly associated with the North Star mine (Brent Thorne and Charles Adan, *pers. commun*.). This material could have come from

Fig. 2. Bodieite overgrowing richelsdorfite on quartz from the Pittsburg-Liberty mine; FOV 0.84 mm. Note that the bodieite is colorless; the green color is from the underlying richelsdorfite.

FIG. 3. Bodieite replaced by montanite on quartz from a dump near the North Star mine; FOV 1.2 mm.

the North Star mine or from one or more other nearby mines, such as the Carisa, Boss Tweed, or Red Rose mines. These mines, noted by Lindgren & Loughlin (1919) as being in the Godiva ore zone, exploited polymetallic (Au-Ag-Cu-Pb) vein deposits emplaced in contact-metamorphosed dolomite. The principle ore minerals were generally galena, cerussite, and enargite and the prominent gangue minerals were quartz and

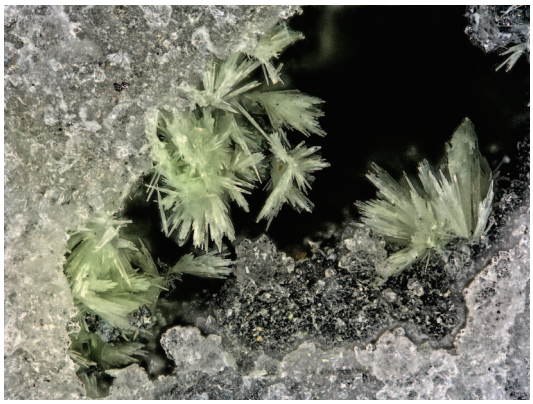

FIG. 4. Bodieite on quartz from the Pittsburg-Liberty mine; FOV 1.14 mm.

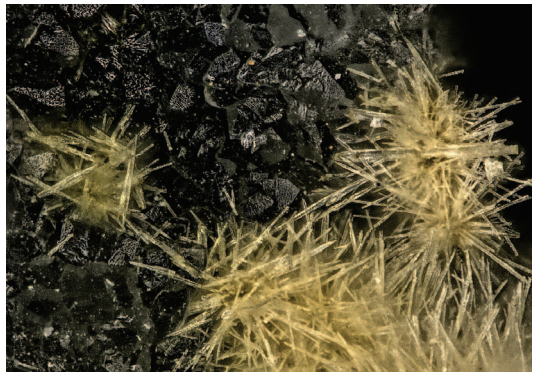

FIG. 5. Bodieite on quartz from the Pittsburg-Liberty mine; FOV 0.68 mm.

baryte. A wide variety of oxidation-zone minerals have been collected from the mine dumps in the area. The recently described new mineral pararaisaite (IMA2017-110; Kampf *et al*. 2018) is from a dump directly associated with the North Star mine.

The Pittsburg-Liberty mine is a former gold mine in the Bodie Hills volcanic field. It exploited a volcanogenic fault-breccia deposit emplaced in granodiorite. The Pittsburg-Liberty was one of the first mines in the Masonic district to be established (1900–1902). In a detailed investigation of the deposits in the Bodie Hills volcanic field, Vikre *et al*. (2015) noted about the Pittsburg-Liberty mine that "Some complex Cu-As-Sb-Fe-Bi-Pb-Ba-Al-Te-S-O phases may have been produced during weathering of sulfide minerals, or may represent submicron intergrowths of sulfide and oxide minerals." Besides the new mineral described here, we have confirmed the presence of the secondary minerals alunite, antlerite, bariopharmacoalumite, bariopharmacosiderite, baryte, bismoclite, bismutite, brochantite, cannonite, cerussite, chalcanthite, chalcomenite, chalcophyllite, clinoclase, conichalcite, cornubite, cornwallite, dussertite, gypsum, jarosite, juabite, mcalpineite, mixite, olivenite, pauladamsite, pharmacosiderite, richelsdorfite, rooseveltite, scorodite, and strashimirite.

We interpret bodieite from both localities as a secondary oxidation-zone mineral. The dump near

TABLE 1. ANALYTICAL DATA (wt.%) FOR BODIEITE

Constituent	Mean	Range	SD	Standard
As_2O_3	1.58	1.50–1.75	0.11	syn. GaAs
Sb_2O_3	0.25	0.09–0.33	0.09	Sb metal
Bi_2O_3	52.14	51.51–52.62	0.40	Bi metal
TeO_2	34.52	34.22–34.80	0.22	Te metal
SO_3	9.40	9.22–9.56	0.15	galena
Total	97.89			

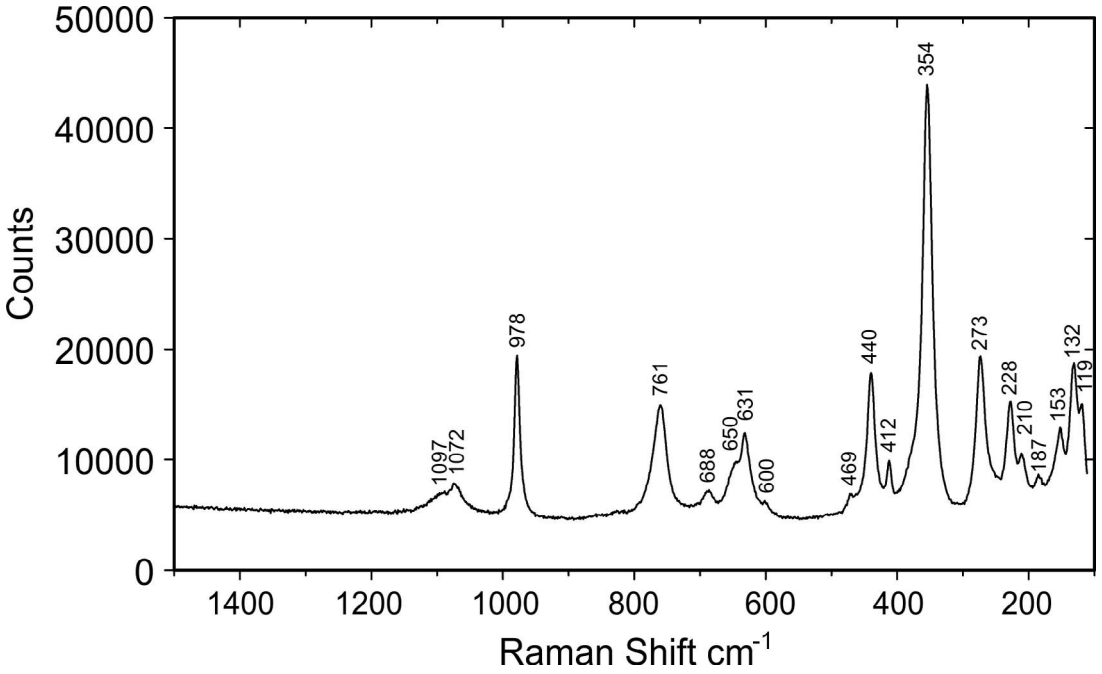

FIG. 6. The Raman spectrum of cotype bodieite (#67483) from the Pittsburg-Liberty mine.

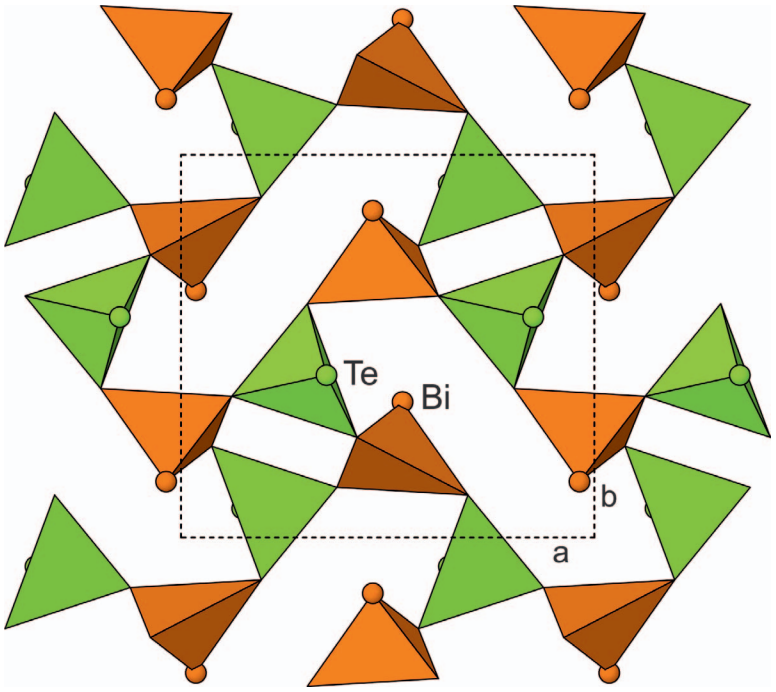

FIG. 7. The $[Bi^{3+}Te^{4+}O_3]^+$ sheet in the structure of bodieite. Three short Te^{4+}–O bonds define a pyramid (green) with Te at its apex. The three short Bi^{3+}–O define a pyramid (orange) with Bi at its apex. The unit cell outline is shown by dashed lines.

TABLE 2. POWDER DATA FOR BODIEITE (ONLY CALCULATED LINES WITH $I \geq 2$ ARE INCLUDED)

I_{obs}	d_{obs}	d_{calc}	I_{calc}	$h\,k\,l$
20	7.31	7.2803	32	0 0 2
		6.6183	2	0 1 1
13	4.583	4.5707	23	$\bar{1}$ 1 2
10	4.188	4.1841	11	1 1 2
9	4.017	4.0144	11	2 0 0
8	3.652	3.6401	11	0 0 4
		3.3425	6	2 1 1
62	3.331	3.3302	60	2 0 2
		3.3265	10	$\bar{1}$ 2 1
		3.3091	3	0 2 2
100	3.243	3.2445	100	1 2 1
13	3.163	3.1648	49	$\bar{1}$ 1 4
20	3.039	3.0326	52	$\bar{2}$ 1 3
3	2.904	2.9068	5	1 1 4
		2.8987	2	$\bar{2}$ 0 4
		2.8458	2	$\bar{1}$ 2 3
		2.7267	7	2 2 0
25	2.716	2.7113	28	0 1 5
		2.6982	3	1 2 3
3	2.611	2.6341	2	$\bar{2}$ 2 2
		2.6001	4	0 2 4
		2.5316	2	2 0 4
		2.5179	2	3 1 0
9	2.487	2.4790	17	$\bar{3}$ 1 2
5	2.436	2.4417	3	0 3 1
		2.4268	4	0 0 6
		2.3908	3	$\bar{2}$ 1 5
		2.3667	2	1 3 0
3	2.287	2.2913	3	3 1 2
		2.2854	2	$\bar{2}$ 2 4
		2.2685	2	$\bar{1}$ 2 5
12	2.213	2.2135	4	$\bar{2}$ 0 6
		2.2061	14	0 3 3
11	2.142	2.1452	19	1 1 6
		2.1261	2	2 1 5
13	2.115	2.1142	10	3 2 1
		2.1074	9	$\bar{2}$ 3 1
		2.0317	3	0 2 6
13	2.0231	2.0213	16	$\bar{1}$ 3 4
4	1.9840	1.9856	7	$\bar{2}$ 3 3
		1.9626	4	2 0 6
15	1.9601	1.9576	2	3 1 4
		1.9545	19	$\bar{4}$ 1 1
21	1.9013	1.9058	21	3 2 3
		1.9016	3	$\bar{2}$ 2 6
		1.8935	4	$\bar{2}$ 1 7
		1.8867	9	0 3 5
9	1.8795	1.8851	7	2 3 3
		1.8713	3	4 0 2
6	1.8582	1.8576	6	0 4 0
		1.8402	3	$\bar{3}$ 2 5
		1.8170	2	$\bar{1}$ 2 7
13	1.8061	1.8030	12	$\bar{3}$ 3 2
		1.7999	3	0 4 2
		1.7761	3	$\bar{1}$ 1 8
4	1.7576	1.7682	2	$\bar{2}$ 3 5
		1.7490	6	$\bar{2}$ 0 8
		1.7270	7	1 2 7
10	1.7223	1.7238	4	4 1 3
		1.7201	2	$\bar{4}$ 1 5
		1.7129	2	$\bar{1}$ 4 3
		1.7058	5	2 1 7
4	1.6878	1.6858	3	2 4 0
		1.6712	2	4 2 2
		1.6687	2	$\bar{4}$ 2 4
17	1.6620	1.6651	6	4 0 4
		1.6609	13	$\bar{4}$ 0 6
		1.6527	6	2 3 5
		1.6458	2	3 1 6
		1.6345	2	0 2 8
6	1.6264	1.6222	5	2 4 2
5	1.5906	1.5919	10	$\bar{3}$ 2 7
		1.5808	4	0 1 9
		1.5793	2	2 0 8
11	1.5719	1.5779	2	$\bar{5}$ 1 2
		1.5731	2	$\bar{3}$ 1 8
		1.5695	5	5 1 0
		1.5681	4	$\bar{4}$ 3 1
		1.5585	2	$\bar{1}$ 4 5
5	1.5307	1.5323	4	$\bar{4}$ 3 3
		1.5300	2	$\bar{3}$ 4 1
		1.5236	2	$\bar{3}$ 3 6
4	1.4992	1.5057	3	3 4 1
		1.4920	6	$\bar{1}$ 2 9
3	1.4729	1.4750	2	0 4 6
		1.4714	3	$\bar{1}$ 3 8
		1.4612	2	1 5 0
6	1.4468	1.4561	3	0 0 10
		1.4401	2	$\bar{1}$ 1 10
		1.4395	6	$\bar{1}$ 5 2
8	1.4291	1.4260	7	3 2 7
		1.3967	3	$\bar{3}$ 4 5
8	1.3876	1.3863	12	$\bar{5}$ 2 5
		1.3766	2	5 1 4
		1.3756	2	1 1 10
8	1.3479	1.3474	4	5 3 0
		1.3447	5	1 5 4
		1.3298	2	$\bar{2}$ 3 9
6	1.3168	1.3183	4	4 3 5
		1.3158	2	$\bar{4}$ 3 7
		1.3149	4	$\bar{6}$ 0 4

TABLE 3. DATA COLLECTION AND STRUCTURE REFINEMENT DETAILS FOR BODIEITE

Diffractometer	Rigaku R-Axis Rapid II
X-ray radiation/power	Mo$K\alpha$ ($\lambda = 0.71075$ Å)/ 50 kV, 40 mA
Temperature	293(2) K
Structural Formula	$Bi^{3+}{}_2(Te^{4+}O_3)_2(SO_4)$
Space group	$I2/a$
Unit cell dimensions	$a = 8.1033(8)$ Å $b = 7.4302(8)$ Å $c = 14.6955(17)$ Å $\beta = 97.771(9)°$
V	876.68(16) Å^3
Z	4
Density (for above formula)	6.555 g/cm^3
Absorption coefficient	46.89 mm^{-1}
F(000)	14.64
Crystal size	40 × 10 × 10 mm
θ range	3.08 to 25.02°
Index ranges	$-9 \le h \le 9$, $-8 \le k \le 8$, $-17 \le l \le 17$
Refls collected/unique	7132/769; $R_{int} = 0.063$
Reflections with $I_o > 2\sigma I$	665
Completeness to θ = 25.02°	99.2%
Refinement method	Full-matrix least-squares on F^2
Parameters/restraints	70/0
GoF	1.157
Final R indices [$I > 2\sigma I$]	$R_1 = 0.0212$, $wR_2 = 0.0330$
R indices (all data)	$R_1 = 0.0275$, $wR_2 = 0.0347$
Extinction coefficient	0.00015(2)
Largest diff. peak/hole	+1.17/–1.41 e/A^3

* $R_{int} = \Sigma|F_o^2 - F_o^2(\text{mean})|/\Sigma[F_o^2]$. GoF = $S = \{\Sigma[w(F_o^2 - F_c^2)^2]/(n-p)\}^{1/2}$. $R_1 = \Sigma||F_o| - |F_c||/\Sigma|F_o|$. $wR_2 = \{\Sigma[w(F_o^2 - F_c^2)^2]/\Sigma[w(F_o^2)^2]\}^{1/2}$; $w = 1/[\sigma^2(F_o^2) + (aP)^2 + bP]$ where a is 0, b is 1.3197, and P is $[2F_c^2 + \text{Max}(F_o^2, 0)]/3$.

the North Star mine yielded a single small specimen that provided the crystals used for EPMA and the solution of the structure. Unfortunately, most of the crystals on this specimen have altered to montanite. Bodieite occurs in vugs in quartz-baryte matrix and is associated with mixite, pyrite, and bismuthinite.

Bodieite has been found on several specimens collected from the lower dump of the Pittsburg-Liberty mine. It occurs in vugs in quartz with embedded crystals of goldfieldite, bismuthinite, and famatinite–luzonite. Other closely associated minerals include baryte, mixite, richelsdorfite, and a poorly crystalline phase containing variable amounts of Cu, Fe, Bi, Te, Sb, and O, possibly related to the pyrochlore supergroup. A 30 × 20 × 8 cm specimen yielded the best crystals of the species, including those pictured in Figures 1 and 2. Besides the species noted above, this specimen has yielded the secondary minerals alunite, antlerite, bariopharmacosiderite, bismutite, cannonite, chalcophyllite, clinoclase, cornwallite, dussertite, juabite, mojaveite, olivenite, pharmacosiderite, rooseveltite, and scorodite.

Physical and Optical Properties

Bodieite occurs in a variety of habits and ranges in color from colorless to yellow to green. It was first noted on a specimen from the North Star mine as olive green blades about 0.3 mm in length. One such crystal was used to solve and refine the structure (see below), but it was found that most other crystals on this specimen had been pseudomorphed by montanite. Crystals from the Pittsburg-Liberty mine range are usually acicular (Figs. 3–5), occasionally steep pyramidal (Fig. 1), and rarely stepped tabular (Fig. 2). They are generally elongate on [001] and exhibit the forms {001}, {110}, {111}, and {11$\bar{1}$}. No twinning was observed. The streak is white, the luster is subadamantine to greasy, and crystals are transparent to translucent. The mineral is nonfluorescent under long- and short-wave ultraviolet light. The Mohs hardness is about 2 based on scratch tests. The tenacity is brittle, the cleavage is fair on {001}, and the fracture is irregular, stepped. The density could not be measured because it is higher than available density liquids and there is not enough material for physical measurement. The calculated density is 6.465 g/cm^3 for the empirical formula and 6.554 g/cm^3 for the ideal formula. The mineral is readily soluble in dilute HCl at room temperature.

Optically, the mineral is biaxial negative with all indices of refraction greater than 2. The Gladstone-Dale relationship (Mandarino 1976) predicts an average index of refraction of 2.123. The $2V$ determined from extinction data on a spindle stage analyzed with the program EXCALIBR (Gunter *et al.* 2004) is 71.5(5)°. Conoscopic observation was not possible, so the dispersion could not be determined. The partially determined optical orientation is $X = \mathbf{b}$.

Raman Spectroscopy

Raman spectra were recorded from all of the samples used in characterizing this mineral and from all the type and cotype specimens, as well as from a number of additional samples. These were obtained using a Renishaw M1000 micro-Raman spectrometer system. Light from a 514.5 nm solid-state laser was focused through a Leica microscope onto the samples. At full power, the laser would supply about 30 mW at the sample, but all spectra were recorded using only 10% power, and samples were always visually inspected before and after spectra were

TABLE 4. ATOM COORDINATES AND DISPLACEMENT PARAMETERS (Å^2) FOR BODIEITE

	x/a	*y/b*	*z/c*	U_{eq}		
Bi	0.03575(4)	0.14587(5)	0.18313(2)	0.01273(12)		
Te	0.14779(7)	0.57599(7)	0.11271(3)	0.01133(16)		
S	1/4	0.1053(4)	0	0.0133(7)		
O1	0.1056(8)	0.2185(9)	0.0109(4)	0.0324(17)		
O2	0.2816(8)	0.9948(8)	0.0836(4)	0.0257(16)		
O3	0.9258(7)	0.2384(8)	0.3051(3)	0.0167(14)		
O4	0.8773(7)	0.3690(7)	0.1228(3)	0.0143(13)		
O5	0.1942(7)	0.3890(7)	0.2008(3)	0.0130(13)		
	U^{11}	U^{22}	U^{33}	U^{23}	U^{13}	U^{12}
Bi	0.01199(19)	0.0112(2)	0.01584(19)	–0.00079(14)	0.00482(13)	–0.00070(15)
Te	0.0107(3)	0.0122(3)	0.0114(3)	0.0010(2)	0.0028(2)	0.0005(2)
S	0.0129(17)	0.0148(18)	0.0130(15)	0	0.0049(13)	0
O1	0.037(4)	0.042(4)	0.018(4)	0.003(3)	0.004(3)	0.024(4)
O2	0.029(4)	0.031(4)	0.018(3)	0.018(3)	0.005(3)	0.005(3)
O3	0.020(4)	0.018(4)	0.013(3)	–0.002(3)	0.006(3)	–0.003(3)
O4	0.010(3)	0.012(3)	0.022(3)	0.007(3)	0.007(3)	0.006(3)
O5	0.011(3)	0.016(4)	0.010(3)	0.005(2)	–0.005(2)	–0.004(2)

recorded, assuring that none were damaged by the laser. Spectral peak positions were periodically calibrated against a silicon (520.5 cm^{-1}) standard and generally varied less than 0.5 cm^{-1}. All spectra were obtained with a dual-wedge polarization scrambler inserted directly above the objective lens to minimize the effects of polarization. Most spectra were recorded from Pittsburg-Liberty mine samples using 20× magnification, resulting in a spot size of about 5 μm. One spectrum from a cotype specimen from the Pittsburg-Liberty mine (#67483) is shown in Figure 6. The Raman spectrum of a crystal from the dump near the North Star mine was obtained from the microprobe sample using 100× magnification resulting in a 1 μm spot size.

All spectra are featureless from 4000 to 1200 cm^{-1}; there is no evidence of OH or H_2O in the mineral. The spectrum in Figure 6 shows the range from 1500 to 100 cm^{-1}. The sharp intense lines reflect the good crystallinity of the sample. The distinct band at 978 cm^{-1} and weak ones at 1097 and 1071 cm^{-1} are in the range typical for minerals containing $(SO_4)^{2-}$ groups. The band at 761 cm^{-1} is consistent with the $(TeO_3)^{2-}$ symmetric stretching mode. Most of the remaining bands are presumably attributable to various stretching and bending modes of $(SO_4)^{2-}$, $(TeO_3)^{2-}$, and $(BiO_3)^{3-}$; however, ambiguities prevent the assignment of specific modes to each of these bands.

Chemical Composition

Six chemical analyses were carried out on crystals from the dump near the North Star mine using a JEOL8200 electron microprobe in WDS mode. The conditions were 15 kV, 5 nA, and 1 μm beam diameter. The crystal exhibited no obvious damage from the beam. No other elements were detected by EDS. Raman spectroscopy and structure analysis indicated the absence of any OH or H_2O. Analytical data are given in Table 1. The empirical formula

TABLE 5. SELECTED BOND DISTANCES (Å) AND ANGLES (°) FOR BODIEITE

Bi–O4	2.208(5)	Te–O3	1.861(5)	S–O1 (×2)	1.467(6)
Bi–O5	2.211(5)	Te–O4	1.890(5)	S–O2 (×2)	1.471(6)
Bi–O3	2.217(5)	Te–O5	1.902(5)	<S–O>	1.469
Bi–O2	2.581(6)	Te–O4	2.698(5)		
Bi–O5	2.599(5)	Te–O1	2.973(6)		
Bi–O1	2.722(6)	Te–O1	3.045(7)		
Bi–O2	2.856(6)	<Te–O>$_{short}$	1.884		
Bi–O3	3.046(6)	<Te–O>$_{long}$	2.905		
<Bi–O>$_{short}$	2.212				
<Bi–O>$_{long}$	2.761				

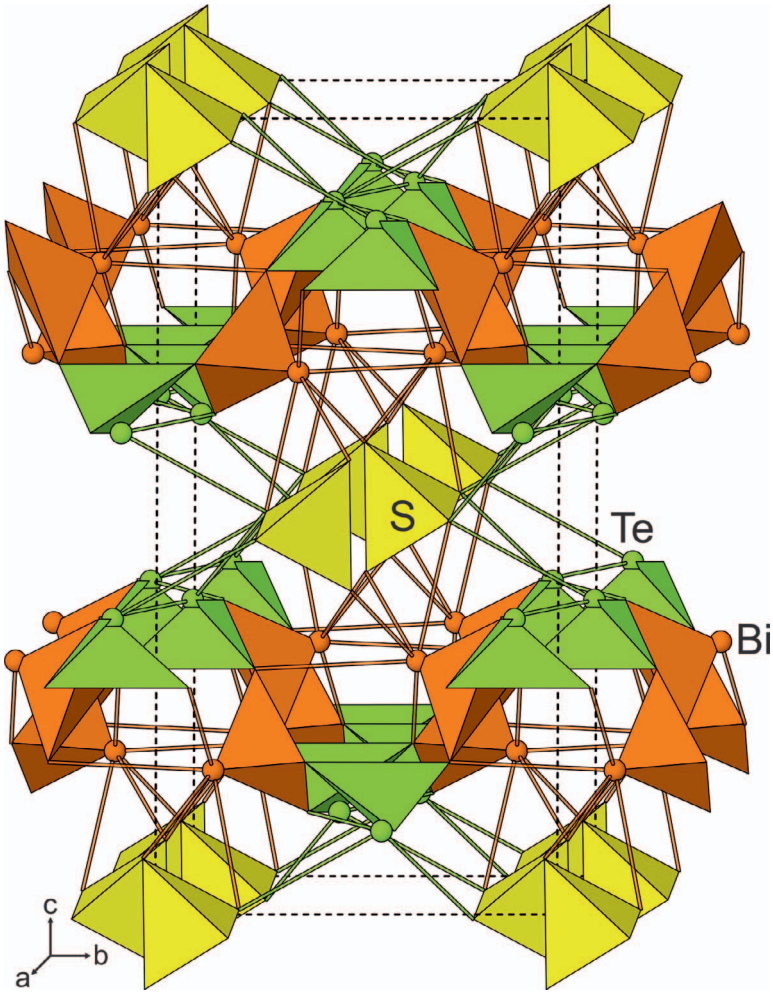

FIG. 8. The structure of bodieite. The longer Te–O and Bi–O bonds are shown as sticks – green and orange, respectively. The unit cell outline is shown by dashed lines.

(based on 10 O atoms) is $(Bi_{1.95}Te_{1.89}As_{0.14}Sb_{0.02})_{\Sigma 4.00}(S_{1.02}O_4)O_6$. The simplified formula is $Bi^{3+}{}_2(Te^{4+}O_3)_2(SO_4)$, which requires Bi_2O_3 53.85, TeO_2 39.89, SO_3 9.25, total 100.00 wt.%.

X-RAY CRYSTALLOGRAPHY

Powder X-ray studies were done using a Rigaku R-Axis Rapid II curved imaging plate microdiffractometer with monochromatized Mo$K\alpha$ radiation (λ = 0.71075 Å). A Gandolfi-like motion on the φ and ω axes was used to randomize the samples. Observed d values and intensities were derived by profile-fitting using JADE 2010 software. Data are given in Table 2. Unit-cell parameters refined from the powder data using JADE 2010 with whole-pattern fitting are a 8.127(4), b 7.444(4), c 14.723(4) Å, β 97.918(9)°, and V = 882.2(7) Å^3.

Single-crystal data were collected using the same diffractometer and radiation noted above. The Rigaku CrystalClear software package was used for processing the structure data, including the application of an empirical absorption correction using the multi-scan method with ABSCOR (Higashi 2001). The structure was solved by direct methods using SIR2011 (Burla *et al.* 2012). Refinement proceeded by full-matrix least-squares on F^2 using SHELXL-2016 (Sheldrick 2015). The cation sites refined to very close to full occupancy by their respective cations and were set to full occupancy in the final refinement. Data collection and refinement details are given in Table 3, atom coordinates and displacement parameters in Table 4, selected bond distances in Table 5,

TABLE 6. BOND-VALENCE ANALYSIS FOR BODIEITE

	Bi	Te	S	Σ
O1	0.19	0.08, 0.07	1.52 ×2↓	1.86
O2	0.27, 0.13		1.50 ×2↓	1.90
O3	0.68, 0.08	1.27		2.03
O4	0.70	1.19, 0.17		2.06
O5	0.69, 0.26	1.15		2.10
Σ	3.00	3.93	6.04	

Values are expressed in valence units. Multiplicity is indicated by ×2↓. Bi^{3+}–O and S^{6+}–O bond valence parameters are from Gagné & Hawthorne (2015); Te^{4+}–O bond valence parameters are from Mills & Christy (2013).

and a bond valence analysis in Table 6. A CIF file that also contains observed and calculated structure factors has been deposited and is available from the Depository of Unpublished Data on the MAC website[1].

Atomic Arrangement

The structure of bodieite is unusual in that it contains two different cations, Bi^{3+} and Te^{4+}, that have stereoactive lone-pair electrons. The coordination of each is characterized by three short cation-oxygen distances and several significantly longer bonds, five for Bi (2.581 to 3.046 Å) and three for Te (2.698 to 3.045 Å). For each, the three short distances are on the same side of the coordination sphere and define a pyramid with the cation as its apex. Bismuth forms short bonds to O3, O4, and O5 (2.208 to 2.217 Å) and Te also forms short bonds to O3, O4, and O5 (1.861 to 1.902 Å). The BiO_3 and TeO_3 pyramids link *via* sharing of O vertices with each O3, O4, and O5 atom being coordinated to one Bi and one Te cation. The resulting linkage results in an undulating sheet of composition $[BiTeO_3]^+$ parallel to {001} (Fig. 7). Bismuth forms two long bonds to O atoms (O3 and O5) within the same sheet and three to the O vertices of SO_4 groups located between the sheets. Tellurium forms one long bond to an O atom (O4) within the same sheet and two to O vertices of SO_4 groups. The relatively weak bonds between the Bi and Te atoms and the interlayer SO_4 groups account for the fair {001} cleavage (Fig. 8). Christy & Mills (2013) provide a detailed discussion of 'secondary' (longer) Te–O bonds in Te^{4+} coordination environments.

Bodieite is structurally quite distinct from any other known mineral, but is isostructural with the synthetic phases $Bi^{3+}{}_2(Te^{4+}O_3)_2(Se^{6+}O_4)$ and $Bi^{3+}{}_2(Se^{4+}O_3)_2(Se^{6+}O_4)$ (Lee *et al*. 2013). In the structural classification of Te oxysalts of Christy *et al*. (2016), bodieite falls into the category of structures with "neso $Te^{4+}X_3$ as part of a larger structural unit that is a layer".

Acknowledgments

Associate Editor Henrik Friis is thanked for sheperding the manuscript. Andrew Christy and an anonymous reviewer are thanked for their constructive comments. At Caltech, the microprobe analyses and Raman studies were funded by grants from the Northern California Mineralogical Association and NSF grant EAR-1322082. The rest of this study was funded by the John Jago Trelawney Endowment to the Mineral Sciences Department of the Natural History Museum of Los Angeles County.

References

Burla, M.C., Caliandro, R., Camalli, M., Carrozzini, B., Cascarano, G.L., Giacovazzo, C., Mallamo, M., Mazzone, A., Polidori, G., & Spagna, R. (2012) *SIR2011*: a new package for crystal structure determination and refinement. *Journal of Applied Crystallography* **45**, 357–361.

Christy, A.G. & Mills, S.J. (2013) Effect of lone-pair stereoactivity on polyhedral volume and structural flexibility: application to $Te^{IV}O_6$ octahedra. *Acta Crystallographica* **B69**, 446–456.

Christy, A.G., Mills, S.J., & Kampf, A.R. (2016) A review of the structural architecture of tellurium oxycompounds. *Mineralogical Magazine* **80**, 415–545.

Gagné, O.C. & Hawthorne, F.C. (2015) Comprehensive derivation of bond-valence parameters for ion pairs involving oxygen. *Acta Crystallographica* **B71**, 562–578.

Gunter, M.E., Bandli, B.R., Bloss, F.D., Evans, S.H., Su, S.C., & Weaver, R. (2004) Results from a McCrone spindle stage short course, a new version of EXCALIBR, and how to build a spindle stage. *The Microscope* **52**, 23–39.

Higashi, T. (2001) *ABSCOR*. Rigaku Corporation, Tokyo, Japan.

Kampf, A.R., Housley, R.M., & Rossman, G.R. (2018) Pararaisaite, the dimorph of raisaite, from the North Star Mine, Tintic, Utah, U.S.A. *Canadian Mineralogist* **56**, this issue.

Lee, E.P., Song, S.Y., Lee, D.W., & Ok, K.M. (2013) New bismuth selenium oxides: syntheses, structures, and characterizations of centrosymmetric $Bi_2(SeO_3)_2(SeO_4)$

[1] Supplementary Data is available from the Depository of Unpublished data on the MAC website (http://mineralogicalassociation.ca/), document "Bodieite, CM56, 18-00046".

and $Bi_2(TeO_3)_2(SeO_4)$ and noncentrosymmetric $Bi(SeO_3)(HSeO_3)$. *Inorganic Chemistry* **52**, 4097–4103.

Lindgren, W. & Loughlin, G.F. (1919) Geology and Ore Deposits of the Tintic Mining District. United States Geological Survey Professional Paper **107**, 276 pp.

Mandarino, J.A. (1976) The Gladstone-Dale relationship – Part 1: derivation of new constants. *Canadian Mineralogist* **14**, 498–502.

Mills, S.J. & Christy, A.G. (2013) Revised values of the bond valence parameters for Te^{IV}–O, Te^{VI}–O and Te^{IV}–Cl. *Acta Crystallographica* **B69**, 145–149.

Ok, K.M., Bhuvanesh, N.S.P., & Halasyamani, P.S. (2001) Bi_2TeO_5: synthesis, structure, and powder second harmonic generation properties. *Inorganic Chemistry* **40**, 1978–1980.

Rossell, H.J., Leblanc, M., Ferey, G., Bevan, D.J.M., Simpson, D.J., & Taylor, M.R. (1992) On the crystal structure of $Bi_2Te_4O_{11}$. *Australian Journal of Chemistry* **45**, 1415–1425.

Sheldrick, G.M. (2015) Crystal Structure refinement with *SHELX*. *Acta Crystallographica* **C71**, 3–8.

Vikre, P.G., John, D.A., du Bray, E.A., & Fleck, R.J. (2015) Gold-silver mining districts, alteration zones, and paleolandforms in the Miocene Bodie Hills volcanic field, California and Nevada. United States Geological Survey Scientific Investigations Report **2015-5012**.

Received July 10, 2018. Revised manuscript accepted August 8, 2018.